

Frequency-Domain Implementation of the Transmitted-Reference Ultra-Wideband Receiver

Sebastian Hoyos and Brian M. Sadler

Abstract—This paper presents a mixed-signal frequency-domain implementation of the autocorrelation receiver used in the detection of ultra-wideband communication signals that are modulated with transmitted-reference signaling. The digital receiver architecture is based on samples provided by an analog-to-digital converter (ADC) in the frequency domain. Among the advantages of the new receiver are the relaxation of the conversion speed achieved by the inherent parallel architecture of the frequency-domain ADC and the flexibility and simplicity of an all-digital receiver architecture that follows the mixed-signal ADC radio front-end. The paper provides the symbol detection formulas and the corresponding system implementation and makes comparisons with the conventional time-domain implementations. Additionally, a time synchronization technique for the new receiver structure is proposed, which makes the receiver insensitive to any time offset at the pulse level. Furthermore, as a particular case of great practical interest, we consider a single bit for the ADC implementation, and we show with experimental results that the resultant frequency-domain mono-bit digital receiver provides a performance gain that increases with the number of frequency samples, when compared with its time-domain counterpart.

Index Terms—All-digital receivers, analog-to-digital (A/D) conversion in the frequency domain, broadband wireless communications, transmitted-reference (TR) communication systems, ultra-wideband (UWB) communications.

I. INTRODUCTION

IMPULSE-RADIO ultra-wideband (UWB) communication systems transmit short and low-power pulses that occupy bandwidths in a frequency interval that ranges from 3.1 to 10.6 GHz, with a minimum instantaneous bandwidth of 500 MHz [1], [2]. This large bandwidth occupancy brings advantages including high data transmission rates, accommodation for a large number of users, and coexistence with the already deployed narrowband and wideband systems. However, significant implementation challenges arise as well due to the use of large bandwidths, stressing key analog and mixed-signal interface devices such as analog-to-digital converters (ADCs). Additional issues include narrowband interference that lowers UWB receiver performance, high-channel frequency selectivity that generates many resolvable multipath components [3], [4], thus compounding the problem of energy capture at the receiver [5], [6], and difficult timing synchronization and acquisition.

Further, the desire to have low energy per pulse drives up the number of pulses per symbol, leading to various direct-sequence-like or multicarrier modulation formats, and further increasing receiver complexity [7]–[10]. Thus, it is of interest to develop low-complexity UWB receivers to achieve low energy consumption, especially for short-range energy-constrained applications.

Although technology based on analog components can accommodate the large UWB signals at the front-end of the receiver, they come at a cost of reduced flexibility in the design. Reduced-complexity analog schemes include the RAKE receiver with a limited number of fingers and possibly suboptimal diversity combining [6], the tunnel diode detector [1], and TR signaling [6], [11], [12].

The TR signaling scheme implemented with an autocorrelation receiver is an old idea that has been revived in the context of UWB. The most basic autocorrelation receiver approach has received special attention for its low-complexity structure where, for each information symbol, both a reference pulse and a modulated information pulse are transmitted. The motivation is that both modulated and unmodulated pulses are equally distorted as they propagate through the channel, so that the unmodulated pulse can be used as a template for calculating the correlation needed to estimate the information symbol. This provides a performance-complexity tradeoff, avoiding costly equalization, channel estimation, and pulse-level synchronization, but at a price in bit-error-rate (BER) performance and throughput due to the transmission of the reference pulse and the use of a noisy template. The synchronization advantage also comes from the transmission of the reference pulse that, independently of time-offset in the received signal, only needs to be delayed by the known value in order to make it align with the modulated pulse. Therefore, TR signaling enables a highly simplified receiver structure, which is generally noncoherent in the sense of not requiring a carrier acquisition step and does not require explicit wideband channel estimation and equalization. Nevertheless, the autocorrelation receiver still requires synchronization at the symbol level.

Analog implementations of the autocorrelation receiver require analog delay lines, which are limited in bandwidth, duration, and programmability; these shortcomings can be overcome in a digital TR receiver. For static channels, it is desirable to use coherent summation of training pulses; this is also facilitated with a digital receiver. However, the implementation of an all-digital UWB autocorrelation receiver requires a gigasample ADC placed at the receiver front-end, which takes samples of the received signal at Nyquist rate. The ADC is a high-speed analog/digital (mixed-signal) device whose state of the art is stressed to cope with the needs of all-digital UWB receivers

Manuscript received August 1, 2005; revised January 6, 2006.

S. Hoyos is with the Berkeley Wireless Research Center, Department of Electrical Engineering and Computer Sciences, University of California at Berkeley, Berkeley, CA 94704-1302 USA (e-mail: hoyos@eecs.berkeley.edu).

B. M. Sadler is with the Army Research Laboratory, AMSRD-ARL-CI-CN, Adelphi, MD 20783 USA (e-mail: bsadler@arl.army.mil).

Digital Object Identifier 10.1109/TMTT.2006.872037

[13]. Current ADCs are limited in the number of bits and sampling speeds and suffer from problems such as ADC saturation due to large narrowband interference. This is of special importance in UWB applications, which are overlaid on existing narrowband systems.

Approaches that address the problems of analog-to-digital (A/D) conversion have been investigated, including those based on multiband signal processing [14]–[19] in which the spectrum of the signal is channelized into several bands by means of a bank of bandpass filters. A/D conversion thus occurs at a much reduced speed for each one of the resultant bandpass signals. In particular, when a single bit is used, the implementation is greatly simplified, and practical monobit UWB digital receivers have significant potential [20], [21]. In the UWB context, it is desirable to channel the signal spectrum into several subbands in order to obtain a parallel ADC implementation at a practical operation speed. However, the implementation of the bank of bandpass filters needed in the multiband processing schemes can be potentially troublesome; problems such as spectrum sharing due to the nonideal characteristics of the bandpass filters will affect the overall system performance. Additionally, since the bank of bandpass filters performs signal decomposition of the received signal, the receiver structure needs to perform signal reconstruction together with information data detection, which increases the system complexity.

In order to solve the difficulties of the multiband ADC approaches, a technique based on signal expansions, that exploits the representation of the received signal in domains different from the time domain, has been proposed [22]. In particular, performing the A/D conversion in the frequency domain has appealing characteristics [23]–[25]. Among the advantages of A/D conversion in the frequency domain are the parallelization of the ADC structure which reduces the overall ADC speed, the avoidance of signal reconstruction since the architecture directly provides samples for discrete-frequency processing, potential for frequency-domain narrowband interference suppression which improves system performance [23], robustness to ADC saturation due to large narrowband interference, and the potential for optimal bit allocation based on reverse water filling, [26].

This paper presents the implementation of an all-digital autocorrelation receiver based on samples provided by an ADC in the frequency domain. The frequency-domain ADC provides a set of N samples of the spectrum of the received signal in every conversion time window of duration T_c seconds. The samples are then used in the digital implementation of the receiver. This approach can be readily generalized to handle multiple delays, multiple pulses per symbol, as well as variable numbers of reference pulses. A simple time-synchronization technique is developed that makes the receiver insensitive to pulse-level time-offsets.

This paper is organized as follows. Sections II-A and II-B provide a brief description of the TR signaling and frequency-domain ADC ideas, respectively. Section III introduces the new receiver structure and addresses time synchronization. Section IV generalizes the receiver architecture to include multiple delays when larger symbol constellations are used. Simulation and experimental results are presented in Section V, and Section VI provides the conclusion.

II. BACKGROUND

A. Signal Model for the TR Receiver

For the simplicity of development, we consider a single-user communication system with just one modulated pulse for each information symbol. Extension to direct-sequence-like schemes [7] have been also considered. A TR communications system may be implemented by transmitting both an unmodulated and modulated pulse with an appropriate time-delay separation [6], [11] given by¹

$$s_{tx}(t) = \sum_{j=-\infty}^{\infty} \sqrt{\frac{E_s}{2}} (w_{tr}(t - jT) + b_j w_{tr}(t - jT - D)) \quad (1)$$

where the pulse $w_{tr}(t)$ is the unitary energy transmitted waveform and, therefore, the total transmitted energy is E_s . The modulated pulse carries the binary information in its polarity through the variable b_j , and it is delayed D seconds with respect to the TR pulse. The received signal can be represented as the convolution of the transmitted signal and the linear channel model as

$$\begin{aligned} s_{rx}(t) &= s_{tx}(t) * h(t) \\ &= \sum_{j=-\infty}^{\infty} \sqrt{\frac{E_s}{2}} (w_{rx}^j(t - jT) + b_j w_{rx}^j(t - jT - D)) + z(t) \\ &= \sum_{j=-\infty}^{\infty} \sqrt{\frac{E_s}{2}} \sum_{l=0}^{L_j-1} \beta^{j,l} (w_{rx}^{j,l}(t - jT - \tau^{j,l}) \\ &\quad + b_j w_{rx}^{j,l}(t - jT - D - \tau^{j,l})) + z(t) \end{aligned} \quad (2)$$

where $*$ is the convolution, $z(t)$ is a white zero-mean Gaussian random process, with two-sided spectral density $N_0/2$ and, for the j th transmitted pulse, the received pulse waveform $w_{rx}^j(t - jT) = w_{tx}(t - jT) * h(t) = \sum_{l=0}^{L_j-1} \beta^{j,l} w_{rx}^{j,l}(t - jT - \tau^{j,l})$ is composed of L_j components arriving at the receive antenna with associated attenuation $\beta^{j,l}$ and time-delay $\tau^{j,l}$. The received multipath components are denoted as $w_{rx}^{j,l}(t)$, which differ from the transmitted pulse $w_{tx}(t)$ due to waveform distortion introduced by the frequency selectivity of the medium, as well as the differentiation induced by the receiving antenna. Additionally, it has been assumed in (2) that both the reference and the modulated pulse have been equally distorted as they pass through the channel. The TR receiver uses the received reference to calculate the decision variable. This is done by bandpass filtering the received signal $s_{rx}(t)$, leading to the bandpass-filtered received signal $r(t)$, and then estimating the autocorrelation at lag D .

B. A/D Conversion in the Frequency Domain

Fig. 1(a) shows the block diagram of the ADC in the frequency domain [22], in which signal projection over the complex exponential functions allows sampling of the continuous-

¹Various modifications are possible, such as employing two spreading sequences, one for the reference bits, and one for the data bits [27]. In a static channel, fewer training pulses may be utilized.

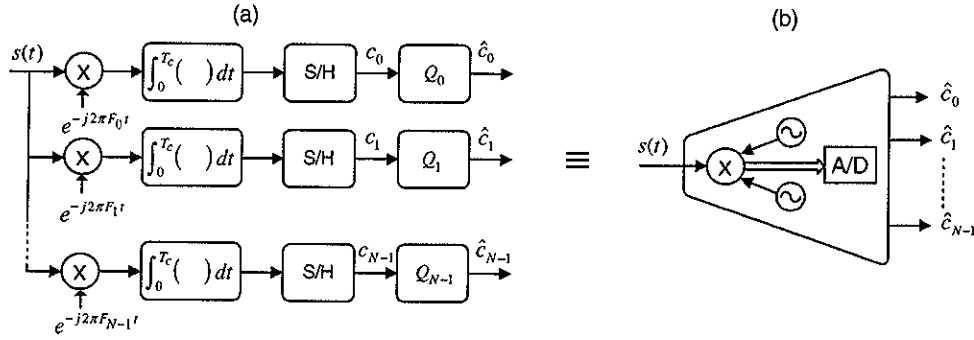


Fig. 1. (a) Block diagram of the ADC in the frequency domain. (b) Block representation of the ADC in the frequency domain.

time signal spectrum at the frequencies F_n , $n = 0, \dots, N-1$, leading to the set of frequency coefficients

$$c_n = \int_0^{T_c} s(t) e^{-j2\pi F_n t} dt, \quad n = 0, \dots, N-1 \quad (3)$$

where T_c is the conversion window time.

The coefficients c_n , $n = 0, \dots, N-1$, are then quantized by a set of quantizers Q_n , $n = 0, \dots, N-1$, which in turn produce the ADC output digital coefficients $\hat{c}_n = Q_n(c_n)$, $n = 0, \dots, N-1$, with associated bit resolutions R_n , $n = 0, \dots, N-1$. The conversion-frequency sample spacing $\Delta F_c = F_n - F_{n-1}$ complies with $\Delta F_c \leq (1/T_c)$ in order to avoid aliasing in the discrete-time domain [14]. Thus, the optimal number of coefficients N necessary to fully sample the signal spectrum with bandwidth W , without introducing time aliasing, is proportional to the time-bandwidth product²

$$N = \left\lceil \frac{W}{\Delta F_c} \right\rceil + 1 \geq \lceil WT_c \rceil + 1 \quad (4)$$

where the operator $\lceil \cdot \rceil$ is used to ensure that N is the closest upper integer that avoids discrete-time aliasing, and the frequencies are allocated uniformly according to

$$F_n = F_{\min} + n\Delta F_c \quad (5)$$

where F_{\min} is the lowest frequency in the range of interest. When $\Delta F_c = (1/T_c)$, (4) turns into an equality, and the discrete-time alias-free condition is satisfied without oversampling the signal spectrum.

The block diagram illustrated in Fig. 1(b) will be used for the representation of the ADC in the frequency domain, regardless of the architecture used for its implementation. Moreover, the impact of the implementation impairments on the frequency-domain ADC has been investigated in [22].

Fig. 2 provides a comparison between conventional time-domain A/D conversion and frequency-domain A/D conversion of the received signal $r(t)$. The conventional time-domain ADC provides the samples $r(nT_s)$, where $F_s = 1/T_s$ is the Nyquist rate, whereas the frequency-domain ADC provides

the frequency samples $R_m(F_n)|_{n=0}^{N-1}$ for the time interval $mT_c \leq t \leq (m+1)T_c$, where T_c is the conversion time. Thus, the frequency domain relaxes the conversion speed by a factor $T_c/T_s = F_s/\Delta F_c$ at the cost of introducing a parallelized ADC structure with N branches, which implies N oscillators, mixers, sample-and-hold devices, and quantizers with the architecture of Fig. 1.³

III. TR SCHEME IN THE FREQUENCY DOMAIN AND ITS SYNCHRONIZATION ISSUES

The samples provided by the frequency-domain ADC can be used in the implementation of the autocorrelation receiver. To see this, we begin by expressing the conventional autocorrelation operation used in the calculation of the decision variable estimate \hat{a} as

$$\hat{a} = \int_0^T r(t)r(t-D)dt \quad (6)$$

which can also be expressed in the frequency domain by using the Fourier analysis

$$\begin{aligned} \hat{a} &= \int_0^T r(t)r(t-D)dt \\ &= \int_{-\infty}^{\infty} R(F)R^*(F)e^{j2\pi DF}dF \\ &= \int_{-\infty}^{\infty} |R(F)|^2 e^{j2\pi DF}dF \\ &\approx \Delta F_c \sum_{n=0}^{N-1} |R(F_n)|^2 e^{j2\pi DF_n} \\ &\quad + \Delta F_c \sum_{n=0}^{N-1} |R(-F_n)|^2 e^{-j2\pi DF_n} \end{aligned} \quad (7)$$

where $R(F)$ denotes the Fourier transform of $r(t)$, the second line follows from the Parseval's theorem, and the error in the approximation of the last line is negligible if the frequencies

²It will be shown that practical values of N are possible. For instance, $N = 4$ is used in the simulation setup of Section V.

³Notice that, although the frequency coefficients c_n are complex-valued in general, only N devices instead of $2N$ are needed if the symmetry of the spectrum of the real-valued received signal is exploited.

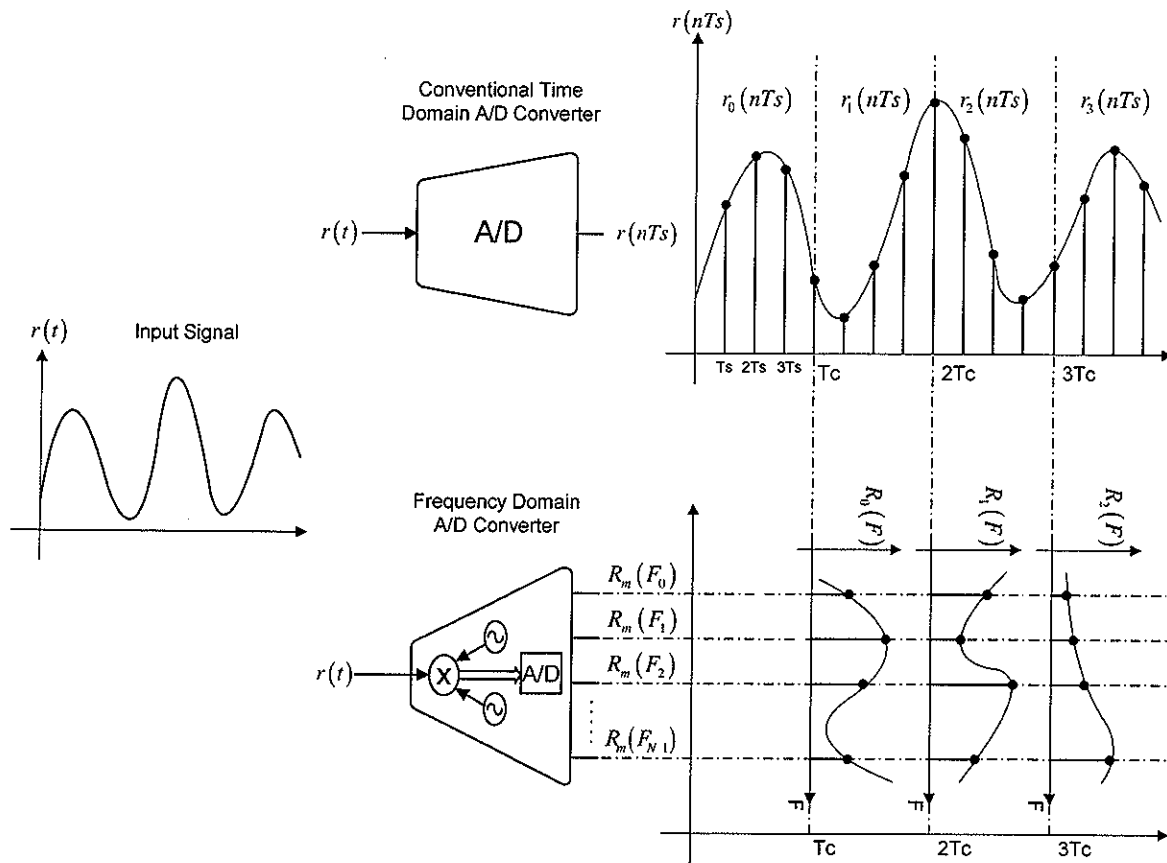


Fig. 2. Illustrative comparison between time- and frequency-domain ADCs.

$F_n|_{n=0}^{N-1}$ satisfy the conditions stated in (4) and other sources of distortion, such as additive white Gaussian noise (AWGN), are more dominant.

In (7), we assume that the symbol period T is equal to the integration time T_c , but this assumption need not hold, as we will show later. Additionally, (7) can be further simplified when the signal is real-valued (i.e., no downconversion is performed at the radio front-end), which leads to $R(F_n) = R^*(-F_n)$. We then have

$$\begin{aligned}
 \hat{a} &\approx \Delta F_c \sum_{n=0}^{N-1} |R(F_n)|^2 e^{j2\pi D F_n} \\
 &\quad + \Delta F_c \sum_{n=0}^{N-1} |R(-F_n)|^2 e^{-j2\pi D F_n} \\
 &= \Delta F_c \sum_{n=0}^{N-1} |R(F_n)|^2 (e^{j2\pi D F_n} + e^{-j2\pi D F_n}) \\
 &= 2\Delta F_c \sum_{n=0}^{N-1} |R(F_n)|^2 \cos(2\pi D F_n). \quad (8)
 \end{aligned}$$

The frequency-domain dual of the autocorrelation receiver reveals some of its most important characteristics. The absolute value square in the frequency samples indicates the non-linear nature of the receiver structure, and the weights $w_n = \cos(2\pi D F_n)|_{n=0}^{N-1}$ account for the time delay D at which the

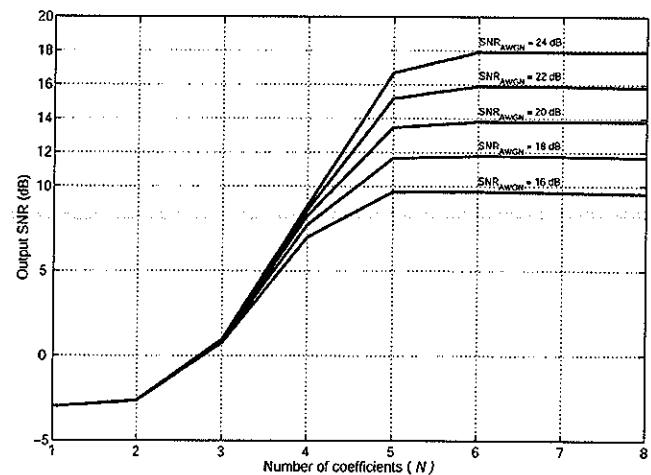


Fig. 3. Impact of truncation error in the receiver output SNR versus the number of frequency coefficients N .

autocorrelation of the received signal is evaluated. If the samples of signal spectrum comply with (4) and the truncation error is negligible, the probability of error of the information estimates in (8) is the same as that for its time-domain equivalent [6], [21]. Truncation error can degrade the performance of the receiver when a lower number of expansion coefficients is used. The impact of truncation error on the receiver output SNR is shown in Fig. 3 parameterized by several input signal

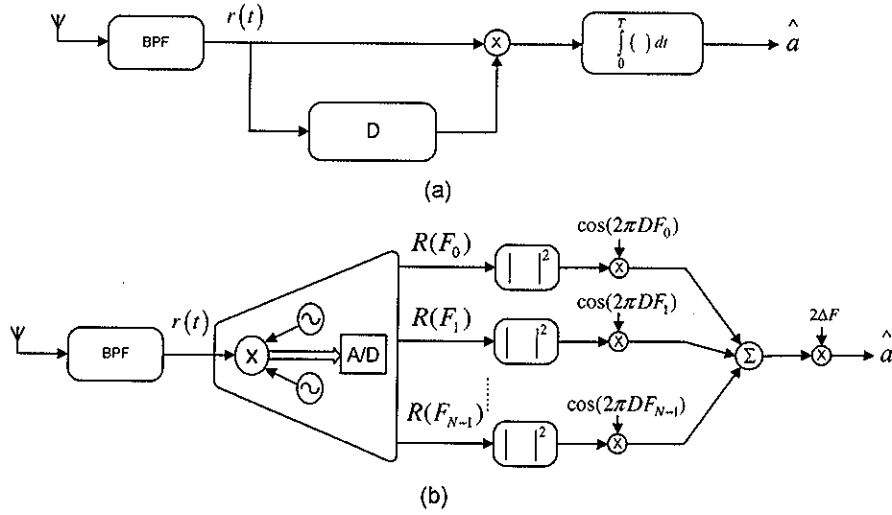


Fig. 4. (a) Conventional analog time-domain transmitted reference receiver. (b) Digital transmitted reference receiver using frequency-domain sampling.

SNRs. Note that the output SNR does not reach the input signal $\text{SNR}_{\text{AWGN}} = 10 \log_{10}(E_b/N_o)$ when truncation becomes negligible, as it would in a matched filter receiver. This is because of the 3-dB overhead introduced by the TR and the penalty introduced by the presence of noise in the received template. Moreover, Fig. 3 shows that, in the low SNR regime, the number of coefficients N can be lowered from that given in (4) ($N = 6$, in this example), because the noise penalty is more dominant than the truncation error.

A. Synchronization

One of the most important advantages of the conventional time-domain autocorrelation receiver is that the synchronization is highly relaxed since the only parameter needed to perfectly align the reference signal and the modulated pulse is the delay D , which is known by the receiver. Thus, only synchronization at the symbol level and not at the pulse level is needed, which can be easily accomplished. It is important that the new implementation of the receiver structure preserves the synchronization advantage of the original receiver. In our approach, there remains an unknown delay with respect to the integration time boundary. Although this synchronization issue seems to be problematic with the structure of Fig. 4, we solve this problem next by a simple modification that exploits the digital representation of the received signal provided by the frequency-domain ADC.

To accomplish this task, we reduce the conversion time to a fraction of the time delay D , i.e., we make $T_c = D/M$, where M is an integer. This restriction is not too strong, and different delays can be accommodated when they are multiples of T_c . As illustrated in Fig. 5, this simple choice of T_c makes the segments that are $D = MT_c$ seconds apart align perfectly with respect to the doublet signal, independent of any time offset. To see that choosing $D = MT_c$ makes the receiver insensitive to time-offsets, Fig. 5 illustrates the case for $M = 3$ ($D = 3T_c$). We show two segment sets: one set is marked 0, 1, 2, 3, 4, 5

that aligns perfectly with the beginning of the doublet, and the other segment set is marked $0^*, 1^*, 2^*, 3^*, 4^*, 5^*$ that has a time offset with respect to the first set. In both sets, the segments $(0, 3)$, $(0^*, 3^*)$, $(1, 4)$, $(1^*, 4^*)$, $(2, 5)$, and $(2^*, 5^*)$ align perfectly with respect to the doublet and can then be combined in the detection formula below. Thus, the receiver structure reduces to simple correlation between the sample frequencies $R_m(F_n)$ with the sample frequencies $R_{m-M}(F_n)$, followed by a summation of M consecutive correlation segments.

In mathematical terms, the received signal is segmented with a window $w_m(t)$ of duration T_c

$$w_m(t) = \begin{cases} 1, & mT_c \leq t \leq (m+1)T_c \\ 0, & \text{elsewhere} \end{cases} \quad (9)$$

$$x_m(t) = x(t)w_m(t) \quad (10)$$

where $m = 0, \dots, M-1$, and the window $w_m(t)$ has been selected as rectangular for the simplicity of the analysis, although other windows with desired characteristics could be used instead. The received signal is then segmented, leading to the segments

$$r_m(t) = r(t)w_m(t). \quad (11)$$

This allows us to express the autocorrelation receiver as follows:

$$\begin{aligned} \hat{a} &= \int_0^T r(t)r(t-D)dt \\ &= \sum_{m=0}^{M-1} \int_{mT_c}^{(m+1)T_c} r_m(t)r_{m-M}(t)dt. \end{aligned} \quad (12)$$

The frequency samples $R_m(F_n)$ associated with the m th segment can be used as follows:

$$\begin{aligned}
\hat{a} &= \sum_{m=0}^{M-1} \int_{mT_c}^{(m+1)T_c} r_m(t)r_{m-M}(t)dt \\
&= \sum_{m=0}^{M-1} \int_{mT_c}^{(m+1)T_c} r_m(t)r_{m-M}(t)dt \\
&= \sum_{m=0}^{M-1} \int_{-\infty}^{\infty} R_m(F)R_{m-M}^*(F)dF \\
&\approx \sum_{m=0}^{M-1} \Delta F \left(\sum_{n=0}^{N-1} R_m(F_n)R_{m-M}^*(F_n) \right. \\
&\quad \left. + \sum_{n=0}^{N-1} R_m(-F_n)R_{m-M}^*(-F_n) \right) \\
&= \sum_{m=0}^{M-1} \Delta F \sum_{n=0}^{N-1} 2\text{Re} \{ R_m(F_n)R_{m-M}^*(F_n) \} \quad (13)
\end{aligned}$$

where $\text{Re}\{\cdot\}$ indicates the real part.

As illustrated in Fig. 5, the receiver is not sensitive to a possible time-offset in the received signal as the corresponding segments are still separated D seconds apart, which is exactly the time delay between the TR and the modulated pulse. However, the receiver still needs to achieve symbol synchronization by finding the range of segments corresponding to a particular information symbol conveyed by the doublet, which is equivalent to determine the initial (t_i) and final (t_f) integration times in the conventional continuous-time approach. In the proposed scheme, the frequency-domain ADC digital outputs can be buffered and then used to obtain symbol-level synchronization. The final detection equation including both a time-offset Δt and uncertainty in the integration times (i.e., uncertainty in the set of segments to be included in the computation), can be expressed as

$$\begin{aligned}
\hat{a} &= \int_{t_i}^{t_f} r(t - \Delta t)r(t - D - \Delta t)dt \\
&= \sum_{m \in \text{doublet}} \int_{mT_c}^{(m+1)T_c} r_m(t - \Delta t)r_{m-M}(t - \Delta t)dt \\
&= \sum_{m \in \text{doublet}} \int_{-\infty}^{\infty} R_{m,\Delta t}(F)R_{m-M,\Delta t}^*(F)dF \\
&\approx \sum_{m \in \text{doublet}} \Delta F \left(\sum_{n=0}^{N-1} R_{m,\Delta t}(F_n)R_{m-M,\Delta t}^*(F_n) \right. \\
&\quad \left. + \sum_{n=0}^{N-1} R_{m,\Delta t}(-F_n)R_{m-M,\Delta t}^*(-F_n) \right) \\
&= \sum_{m \in \text{doublet}} \Delta F \sum_{n=0}^{N-1} 2\text{Re} \{ R_{m,\Delta t}(F_n)R_{m-M,\Delta t}^*(F_n) \}. \quad (14)
\end{aligned}$$

A larger number of stored segments will enhance the performance by enabling a search over multiple symbol boundaries and can directly feed a decoder. On the other hand, in a time-domain analog implementation, the symbol-level synchronization requires shifting the integration start/stop times and may therefore require a serial search with a long preamble.

IV. FREQUENCY-DOMAIN AUTOCORRELATION RECEIVER FOR GENERALIZED TR SIGNALING

Among the disadvantages of the TR signaling scheme and its autocorrelation receiver are the penalty associated with the use of a noisy template and a 3-dB loss in performance due to the transmission of a reference pulse with half of the total transmission power. The penalty associated with the noisy template can be mitigated by using a cleaner template obtained from averages over several received pulses [6]. The 3-dB loss can be lowered by increasing the number of information bits for every TR pulse. This implies an increment in the constellation size of the modulation format, which, in turn, involves the use of multiple delays that separate the modulated pulses from the reference. The discrete-frequency-domain implementation follows naturally from the analysis of the previous sections. Additionally, in order to make the receiver performance insensitive from any time-offset in the received signal, all of the delays $D_l|_{l=1}^L$ are multiples of a reference delay D (i.e., $D_l = lD$, $l = 1, \dots, N$), and the received signal is segmented at a fraction of the reference delay D (i.e., $T_c = D/M$). The information variable estimate at the l th lag is evaluated as

$$\begin{aligned}
\hat{a}_l &\approx \sum_{m=0}^{LM-1} \Delta F \left(\sum_{n=0}^{N-1} R_m(F_n)R_{m-lM}^*(F_n) \right. \\
&\quad \left. + \sum_{n=0}^{N-1} R_m(-F_n)R_{m-lM}^*(-F_n) \right) \\
&= \sum_{m=0}^{LM-1} \Delta F \sum_{n=0}^{N-1} 2\text{Re} \{ R_m(F_n)R_{m-lM}^*(F_n) \} \quad (15)
\end{aligned}$$

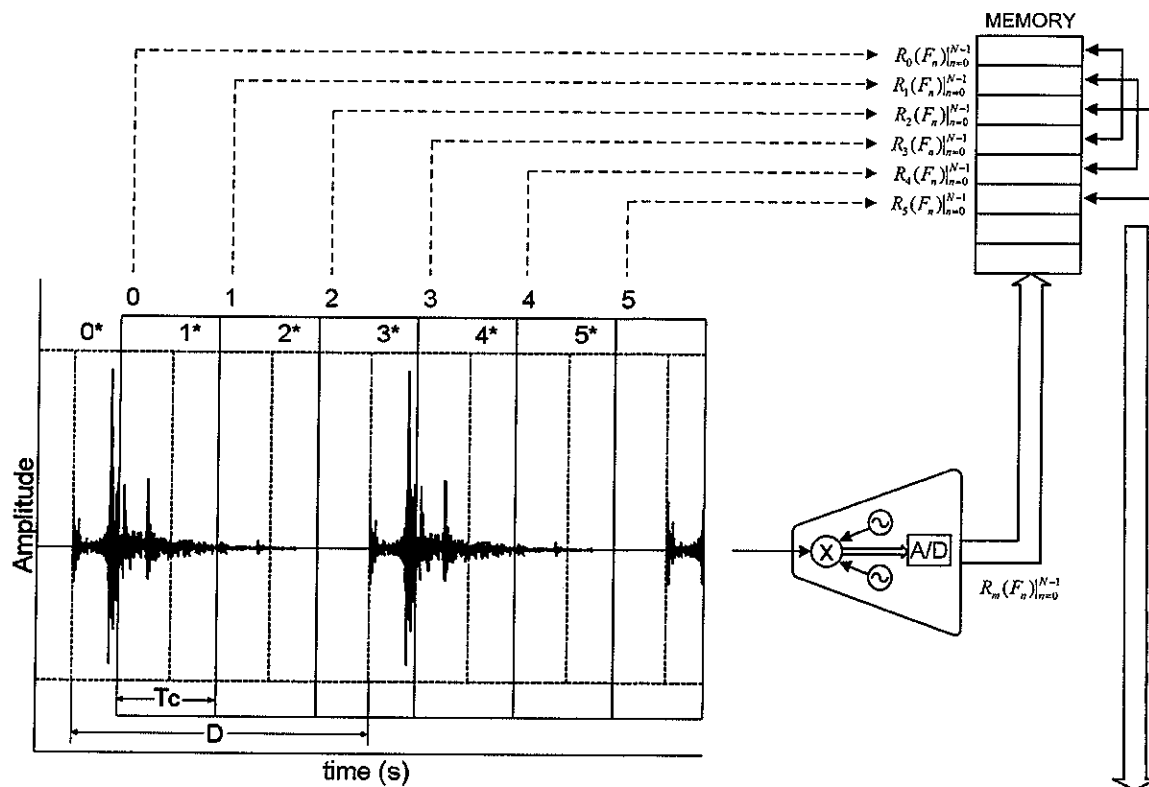
where once again the error of the approximation is negligible when the frequency samples satisfy the frequency sampling condition stated in Section II-B. The BER of the frequency-domain implementation is the same of the conventional time-domain implementation, a result that has been corroborated through system simulations.

Multiple delays can also be used to provide multiple-access capabilities in a time-hopping impulse-radio scheme [7]. In this scenario, the multiuser detection algorithm needs to be implemented with the frequency-domain samples [28]. If all of the delays are multiples of a reference delay, the synchronization problem is simplified, as explained above.

V. SIMULATIONS

Here, we simulate the new receiver architecture and the conventional time-domain receiver in order to provide a comparison between the two approaches. An ideal simulation in AWGN is first presented, and a second simulation that takes into account the effect of real multipath channels is also considered.

The second derivative of Gaussian pulse $w_{tx}(t) = [1 - 4\pi[(t - T_w)/2]/(T_w/2)]^2 \exp(-2\pi[(t - T_w)/2]/(T_w/2)]^2)$



$$\hat{a} = \sum_{n=0}^{M-1} \Delta F_c \sum_{m=0}^{N-1} 2 \operatorname{Re} \{ R_m(F_n) \cdot R_{m-M}^*(F_n) \} = \Delta F_c \sum_{n=0}^{N-1} 2 \operatorname{Re} \{ R_3(F_n) \cdot R_0^*(F_n) + R_4(F_n) \cdot R_1^*(F_n) + R_5(F_n) \cdot R_2^*(F_n) \}$$

Fig. 5. Receiver synchronization is simplified by choosing $T_c = D/M$, which guarantees that the receiver performance is not affected by random offset of the integration time boundary.

is used for carrying the information symbols using the TR signaling scheme, with pulse duration T_w . A full-resolution frequency-domain ADC that relaxes the conversion speed by a factor of N (i.e., $T_c = NT_s = N/F_s$, where $F_s = 1/T_s$ is the Nyquist rate) is used for obtaining the digital representation of the received signal in AWGN. Fig. 6 shows the BER versus $\text{SNR} = 10 \cdot \log_{10}(E_b/N_o)$, where E_b is the energy per information bit and $N_o/2$ is the two-sided power spectral density. Note that the pulse bandwidth is inversely proportional to its duration T_w . Thus, the number of time samples taken at a rate $F_s = 1/T_s$ needed to comply with Nyquist criteria is fixed and given by $T_w/T_s \approx 4$, since changing T_w will produce a proportional change in T_s . Therefore, we make $T_c = T_w$ and set $N = 4$ for the simulations. Note that the simulations are independent of D as long as $D > T_w$, which avoids interpulse interference. BER results for the improved autocorrelation receiver using received reference pulse averaging are shown. The plot shows the BER for averages of 3 and 5, and the case of the simple implementation with no averaging is also shown for comparison. Given the remarkable gains from the averaging of template signals [6], a digital implementation is of great practical interest, whereas the analog time-domain implementation requires a bank of analog delays with analog summing.

Fig. 7 shows a comparison between a single-bit (mono-bit) implementation of the time- and frequency-domain approaches

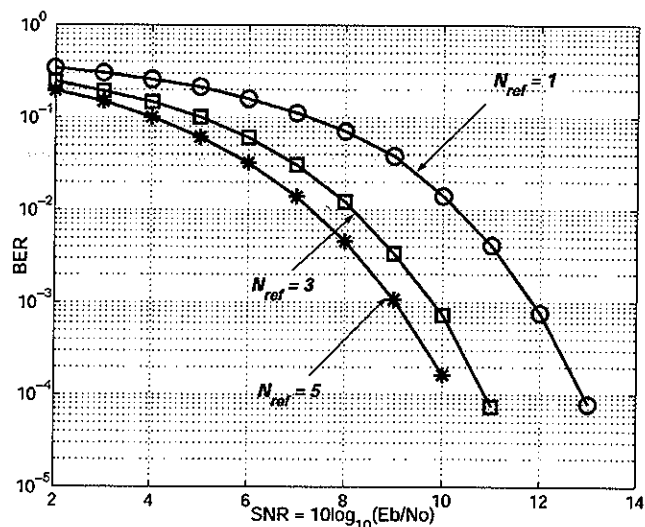


Fig. 6. Proposed receiver BER performance, incorporating reference pulse averaging over N_{ref} pulses, to improve the autocorrelation template. The number of frequency samples in $N = 4 \approx T_w/T_s$.

under the same conditions of the previous simulation. The mono-bit approach is a case of high interest since it greatly relaxes the complexity of the ADC. Here, the frequency sam-

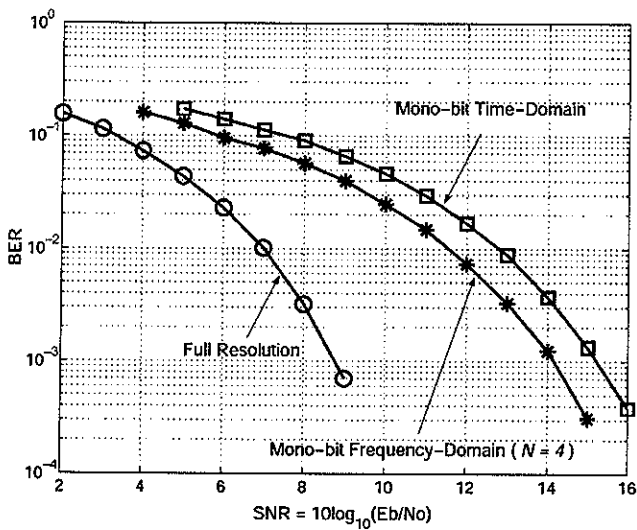


Fig. 7. BER comparison between mono-bit time-domain and mono-bit frequency-domain TR receivers in AWGN.

ples $R_m(F_n)$ are quantized by a single-bit quantizer, leading to $\bar{R}_m(F_n) = \text{sign}(\text{Re}\{R_m(F_n)\}) + j * \text{sign}(\text{Im}\{R_m(F_n)\})$, where $\text{Re}\{\cdot\}$ and $\text{Im}\{\cdot\}$ are the real and imaginary parts, respectively. The plots show that the mono-bit receiver, which is based on a frequency-domain ADC with $N = 4$, outperforms its mono-bit time-domain counterpart. Here, the proposed receiver provides four complex-valued bits every T_c seconds, i.e., 8 b per T_c , whereas the mono-bit time-domain ADC yields four (real-valued) bits per T_c seconds. However, the proposed receiver samples in parallel at the same instant, thus sampling at an overall rate that is four times slower than the conventional time-domain architecture, and yields a 1-dB BER improvement @BER = 10^{-4} . Additionally, better performance can be attained if optimal bit allocation is used with a reasonable tradeoff in complexity, since more than a single bit will be allocated in the frequency samples with larger energy.

In order to consider the effect of multipath channels, measured pulses were used to simulate the frequency- and time-domain mono-bit receivers. As a final performance evaluation of the digital receivers presented in this paper, we utilize a UWB measurement database.⁴ A total of 1699 pulses measured in an office, a townhouse, and a chamber, with distances between transmit and receive antennas in the range from 1.05 to 14.8 m, with both line-of-sight and nonline-of-sight, were used to calculate the average BER of the TR digital receivers. AWGN was added to the measured pulses to set the simulation SNR. Fig. 8 shows the simulation results, where the new receiver architecture based on the mono-bit frequency-domain ADC shows a performance gain when compared with its time-domain counterpart. The gain can also be explained as oversampling in the frequency domain due to the parallel path processing. This gain increases with the number of frequency samples, which encompasses a tradeoff between gain and complexity for low-resolution applications. Fig. 9 shows the performance improvement of

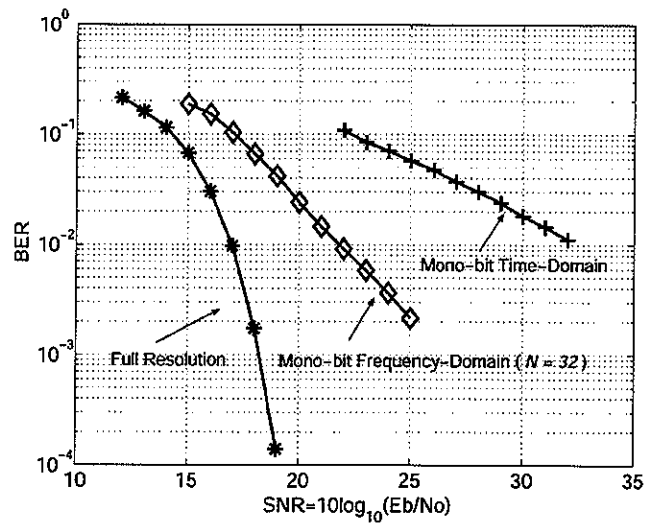


Fig. 8. BER comparison between the mono-bit time-domain and the mono-bit frequency-domain receivers using experimentally collected UWB pulses in an indoor environment.

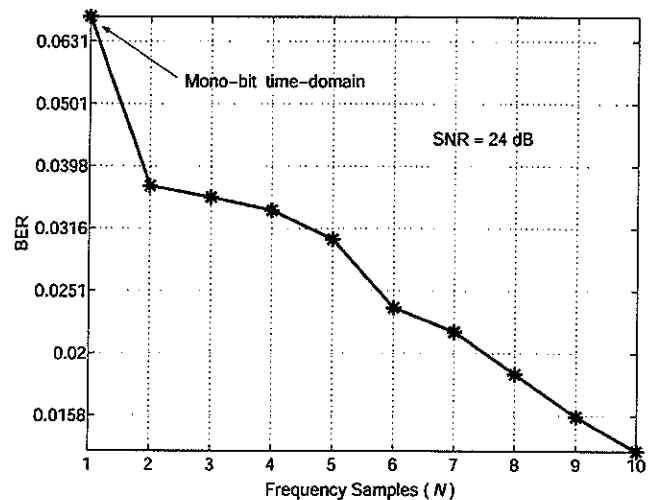


Fig. 9. Increasing the number of frequency-domain samples enhances the BER performance of the proposed receiver. This example is based on measured indoor UWB pulses.

the mono-bit frequency-domain implementation versus a practical number of frequency samples ($1 \leq N \leq 10$) for a fixed SNR = 24 dB, where the same database has been used for calculating the average BER.

VI. CONCLUSION

This paper introduced a discrete-frequency implementation of the autocorrelation receiver used for the estimation of information symbols in TR signaling. The receiver architecture uses the frequency samples provided by an ADC in the frequency domain. A/D conversion in the frequency domain is an emerging technology with multiple benefits, including the relaxation of the conversion speed due to the inherent parallel architecture of the ADC structure, narrowband interference excision that can be directly implemented in the frequency domain, robustness to ADC saturation due to large narrowband interference, and the

⁴[Online]. Available: http://ultra.usc.edu/New_Site/database.html

possibility of using optimal bit allocation to reduce the quantization error.

The proposed TR receiver has low computational complexity and benefits from the parallel digital streams coming from the ADC. Transferring quantization error from the time to the frequency domain is beneficial for UWB signals. Additionally, the new approach outperforms the traditional time-domain digital implementations when a single bit is used in the A/D conversion of the received signal. This gain increases with the number of frequency samples. This result is of special interest since, when a single bit is used in the implementation, the ADC structure complexity is greatly reduced.

The implementation of techniques to combat narrowband interference and performance comparison and analysis with larger number of bits ($b > 1$) are future works of interest.

REFERENCES

- [1] J. D. Taylor, *Introduction to Ultra-Wideband Systems*. Ann Arbor, MI: CRC, 1995.
- [2] "Revision of part 15 of the Commission's rule regarding ultra-wideband transmission," FCC, Washington, DC, 1st Rep. and Order, 2002.
- [3] R. J. Crammer, R. A. Scholtz, and M. Z. Win, "On the analysis of UWB communications channels," in *Proc. MILCOM*, Oct./Nov. 1999, vol. 2, pp. 1191–1195.
- [4] M. Z. Win and R. A. Scholtz, "On the energy capture of ultrawide bandwidth signals in dense multipath environments," *IEEE Commun. Lett.*, vol. 2, no. 9, pp. 245–247, Sep. 1998.
- [5] D. Cassioli, M. Z. Win, F. Vatalaro, and A. F. Molisch, "A study of the ultra-wideband wireless propagation channel and optimum UWB receiver design," in *Proc. IEEE Int. Commun. Conf.*, New York, NY, Apr. 2002, vol. 2, pp. 763–767.
- [6] J. D. Choi and W. E. Stark, "Performance of ultra-wideband communications with suboptimal receivers in multipath channels," *IEEE J. Sel. Areas Commun.*, vol. 20, no. 9, pp. 1754–1766, Dec. 2002.
- [7] M. Z. Win and R. A. Scholtz, "Ultra-wide bandwidth time-hopping spread-spectrum impulse radio for wireless multiple-access communications," *IEEE Trans. Commun.*, vol. 48, no. 4, pp. 679–689, Apr. 2000.
- [8] F. Ramirez-Mireles, "Performance of ultrawideband SSMA using time hopping and M -ary PPM," *IEEE J. Sel. Areas Commun.*, vol. 19, no. 4, pp. 1186–1196, Jun. 2001.
- [9] J. R. Foerster, "The performance of a direct sequence spread ultra wideband systems in the presence of multipath, narrowband interference, and multiuser interference," in *Proc. IEEE Ultra Wideband Syst. Technol. Conf.*, Baltimore, MD, May 2002, pp. 87–92.
- [10] B. M. Sadler and A. Swami, "On the performance of episodic UWB and direct-sequence communication systems," *IEEE Trans. Wireless Commun.*, vol. 3, no. 6, pp. 2246–2255, Nov. 2004.
- [11] R. Hoctor and H. Tomlinson, "Delay-hopped transmitted-reference RF communications," in *Proc. IEEE Ultra Wideband Syst. Technol. Conf.*, Baltimore, MD, May 2002, pp. 265–269.
- [12] S. Hoyos, B. M. Sadler, and G. R. Arce, "Dithering and sigma-delta modulation in mono-bit digital receivers for ultra-wideband communications," in *Proc. IEEE Ultra Wideband Syst. Technol. Conf.*, Reston, VA, Nov. 2003, pp. 71–75.
- [13] R. H. Walden, "Analog-to-digital converter survey and analysis," *IEEE J. Sel. Areas Commun.*, vol. 17, no. 3, pp. 539–550, Apr. 1999.
- [14] A. Papoulis, "Generalized sampling expansion," *IEEE Trans. Circuits Syst.*, vol. CAS-24, no. 11, pp. 652–654, Nov. 1977.
- [15] S. R. Velazquez, T. Q. Nguyen, and S. R. Broadstone, "Design of hybrid filter banks for analog/digital conversion," *IEEE Trans. Signal Process.*, vol. 46, no. 4, pp. 956–967, Apr. 1998.
- [16] W. Namgoong, "A channelized digital ultra-wideband receiver," *IEEE Trans. Wireless Commun.*, vol. 3, no. 5, pp. 502–510, May 2003.
- [17] R. M. Gray, "Oversampled sigma-delta modulation," *IEEE Trans. Commun.*, vol. COM-35, no. 5, pp. 481–489, May 1987.
- [18] P. Aziz, H. Sorensen, and J. Van der Spiegel, "Multiband sigma-delta modulation," *Electron. Lett.*, vol. 29, no. 9, pp. 760–762, Apr. 1993.
- [19] I. Galton and H. T. Jensen, "Delta-sigma modulator based A/D conversion without oversampling," *IEEE Trans. Circuits Syst. II: Analog Digit. Signal Process.*, vol. 42, no. 12, pp. 773–784, Dec. 1995.
- [20] I. D. O'Donnell, M. S. W. Chen, S. B. T. Wang, and R. W. Brodersen, "An integrated, low power, ultra-wideband transceiver architecture for low-rate, indoor wireless systems," presented at the IEEE CAS Wireless Commun. Networking Workshop, Pasadena, CA, Apr. 2002.
- [21] S. Hoyos, B. M. Sadler, and G. R. Arce, "Mono-bit digital receivers for ultra-wideband communications," *IEEE Trans. Wireless Commun.*, vol. 4, no. 4, pp. 1337–1344, Jul. 2005.
- [22] S. Hoyos and B. M. Sadler, "Ultra-wideband analog to digital conversion via signal expansion," *IEEE Trans. Veh. Technol.*, vol. 54, no. 9, pp. 1609–1622, Sep. 2005.
- [23] S. Hoyos, B. M. Sadler, and G. R. Arce, "Broadband multicarrier communications receiver based on analog to digital conversion in the frequency domain," *IEEE Trans. Wireless Commun.*, vol. 5, no. 2, pp. 652–661, Mar. 2006.
- [24] H.-J. Lee and D. S. Ha, "Frequency domain approach for CMOS ultra-wideband radios," in *Proc. IEEE Computer Soc. Annu. Symp. VLSI*, Feb. 2003, pp. 236–237.
- [25] H.-J. Lee, D. S. Ha, and H.-S. Lee, "A frequency-domain approach for all-digital CMOS ultra-wideband receivers," in *Proc. IEEE Ultra Wideband Syst. Technol. Conf.*, Reston, VA, Nov. 2003, pp. 86–90.
- [26] T. M. Cover and J. A. Thomas, *Elements of Information Theory*. New York: Wiley, 1991.
- [27] D. Xu and B. M. Sadler, "Code aided near full rate multiuser tr-uwb systems," in *Proc. 7th IEEE Int. Signal Process. Advances Wireless Commun. Workshop*, Jun. 2005, pp. 980–984.
- [28] Z. Xu, J. Tang, and P. Liu, "Frequency-domain estimation of multiple access ultra-wideband signals," in *Proc. IEEE Stat. Signal Process. Workshop*, St. Louis, MO, Sep. 28–Oct. 1, 2003, pp. 65–68.



Sebastian Hoyos was born in Cali, Colombia, in 1975. He received the B.S. degree from the Pontificia Universidad Javeriana (PUJ), Bogota, Colombia, in 2000, and the M.S. and Ph.D. degrees from the University of Delaware, Newark, in 2002 and 2004, respectively, all in electrical engineering.

He was with Lucent Technologies from 1999 to 2000 as a Technical Manager and Sales Engineer for the Andean region in South America. Simultaneously, he was an Adjunct Professor with PUJ, where he lectured on microelectronics and control

theory. In fall 2000, he joined the Department of Electrical and Computer Engineering, University of Delaware. During his time there, he worked under the PMC-Sierra Inc., the Delaware Research Partnership Program, and the Army Research Laboratory (ARL) Collaborative Technology Alliance (CTA) in Communications and Networks. In fall 2004, he joined the Department of Electrical Engineering and Computer Sciences, University of California, Berkeley, as a Postdoctoral Researcher with the Berkeley Wireless Research Center. He has carried out industrial consulting with Conexant Systems Inc., Red Bank, NJ. His research interests include communication systems, wireless communications, robust signal processing, and mixed-signal high-speed processing and circuit design.



Brian M. Sadler received the B.S. and M.S. degrees from the University of Maryland at College Park and the Ph.D. degree from the University of Virginia, Charlottesville, all in electrical engineering.

He is a Senior Research Scientist with the Army Research Laboratory (ARL), Adelphi, MD. He was a Lecturer with the University of Maryland at College Park and has been lecturing at The Johns Hopkins University, Laurel, MD, since 1994 on statistical signal processing and communications. His research interests include signal processing for

mobile wireless and ultra-wideband systems and sensor signal processing and networking. He is on the Editorial Board for the *EURASIP Journal on Wireless Communications and Networking*.

Dr. Sadler is an associate editor for the *IEEE SIGNAL PROCESSING LETTERS*, was an associate editor for the *IEEE TRANSACTIONS ON SIGNAL PROCESSING*, and was a guest editor for a Special Issue on Military Communications of the *IEEE JOURNAL ON SELECTED AREAS OF COMMUNICATIONS*.